SUPPLEMENTARY DATA

Supplementary Table 1. Specific primers used for PCR.

Primers	**Forward**	**Reverse**
RILP-RT-PCR(rat)	5' TCAAGGAGGTGACAGACAGA 3'	5' GAGCATCTCTCGCTGGAAATA 3'
RILP-qPCR(rat)	5' CTCAAGGAGGAGTTGGCATATT 3'	5' GCCTTGATCTTTCTCCTCTGTT 3'
RILP-qPCR(mouse)	5' GAACAGAGCTTGGAACCTGAT 3'	5' CATCTTCCTTGTCGTTGGAGAG 3'
Ins1-qPCR(mouse)	5' CCTTCAGACCTTGGCGTTGG 3'	5' CGAGGTGGGCCTTAGTTGCA 3'
Ins2-qPCR(mouse)	5' ACCCACAAGTGGCACAACTG 3'	5' AGGGGTAGGCTGGGTAGTG 3'
β-actin- qPCR(mouse)	5' GATCTGGCACCACACCTTCT 3'	5' GGGGTGTTGAAGGTCTCAAA 3'
GAPDH-qPCR(rat)	5' GGAGAAACCTGCCAAGTATGA 3'	5' TTGAAGTCACAGGAGACAACC 3'
Rab26-RT-PCR(mouse)	5' ACTCTACTCAAGACCGTGTGG 3'	5' TCCATGAAAGGTAGCCCATACT 3'

SUPPLEMENTARY DATA

Supplementary Table 2. The list of sequences for shRNA.

Primers	**shRNA**
shRILP-1#	5’ CAGCTATGC AGGAGGCTTA 3’
shRILP-2#	5’ CAGAGCTTGGAACCTGATG 3’
shRILP-3#	5’ GTCCAAGGTGTTTCTGCTG 3’
shRab7-1#	5’ TTCCCTGAACCCATCAAAC 3’
shRab7-2#	5’ CCAGTACAAAGCCACAATA 3’
shRab7-3#	5’ GAAGTTCAGTAACCAGTAC 3’
shRab26-1#	5’ GGCATCGACTTCCGGAATAAA 3’
shRab26-2#	5’ CAGGCTGCATGACTATGTTAA 3’
shRab26-3#	5’ GCTCATGCTGCTAGGGAACAA 3’
shRab26-4#	5’ GCTTCAGGCTGCATGACTATG 3’

SUPPLEMENTARY DATA

Supplementary Figure 1. Islets from mice were efficiently infected with recombinant adenovirus. (A), Immuno-staining with insulin/proinsulin antibody in the mouse islets were transfected with Ad-vector adenovius. (B), Immuno-staining with insulin/proinsulin antibody in the mouse islets were transfected with Ad-RILP adenovius. (C), Western-blot showed the expression of RILP in the mouse islets transfected with recomninant adenovius.

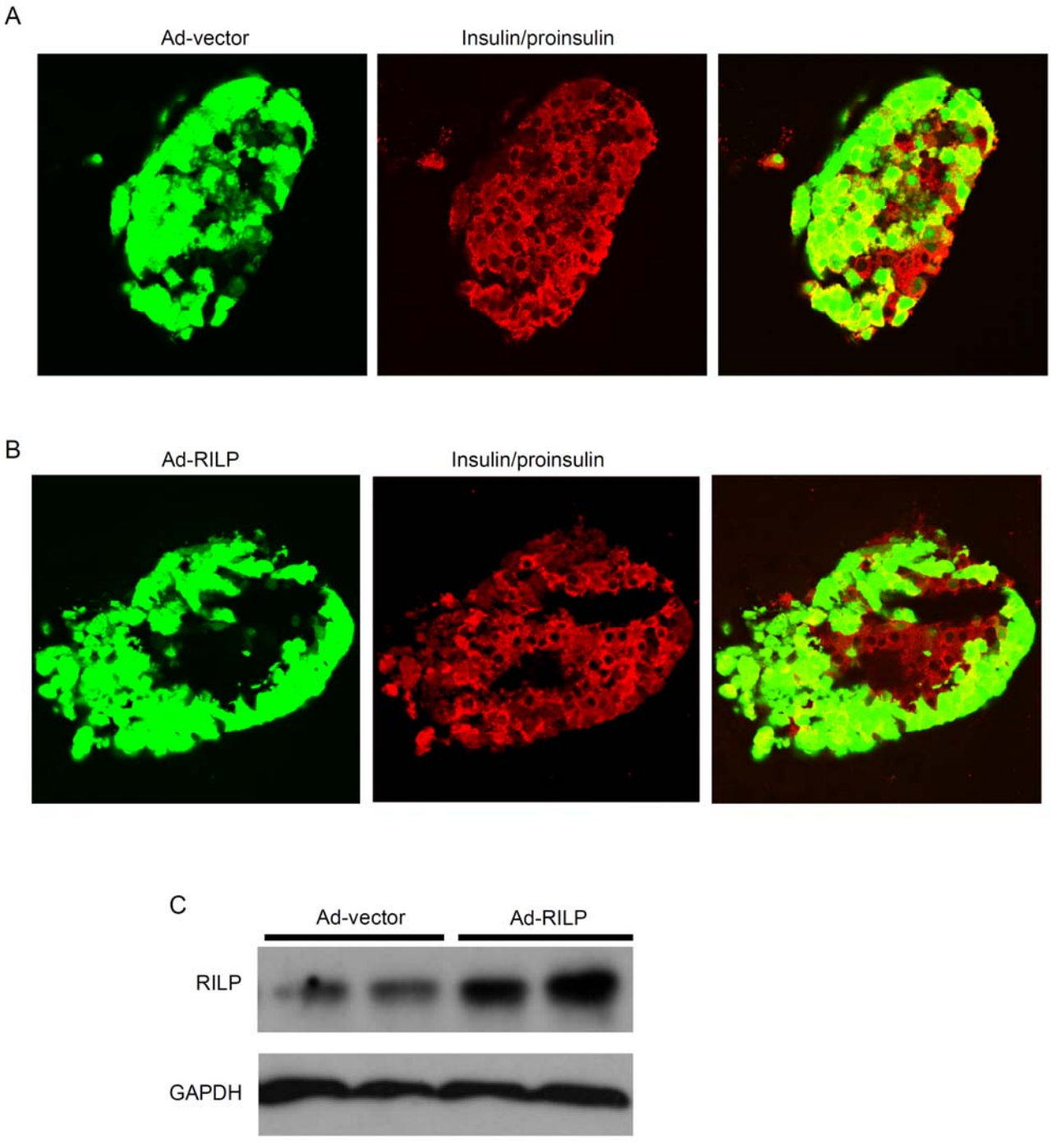

SUPPLEMENTARY DATA

Supplementary Figure 2. (A), Streptozotocin injection results in the increase of the plasma glucose level in mice. (B), qPCR products from the islets of db/db mice to demonstrate the expression of RILP.

A

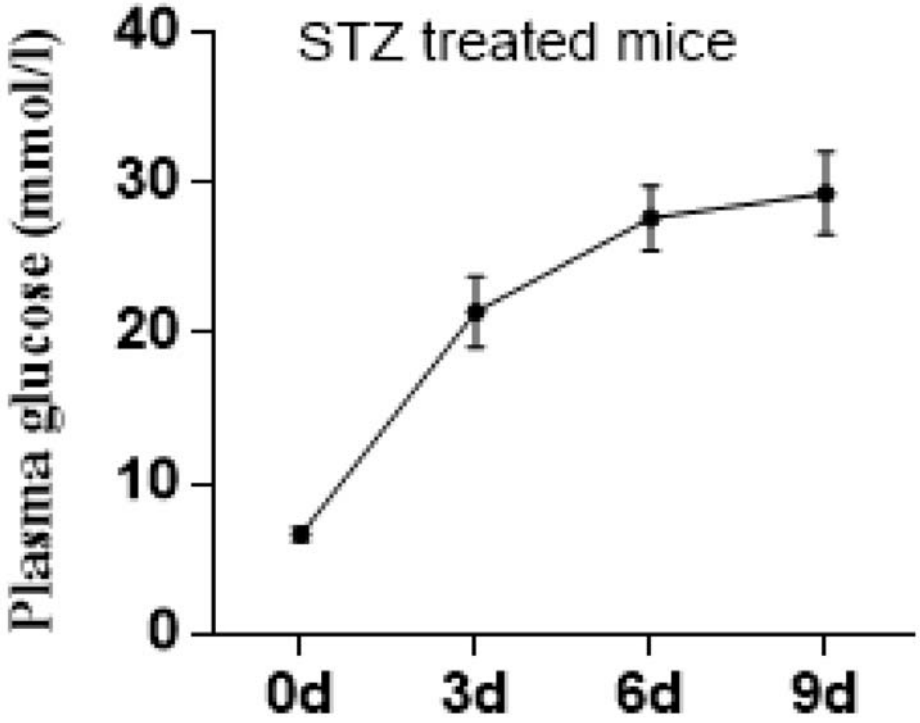

B

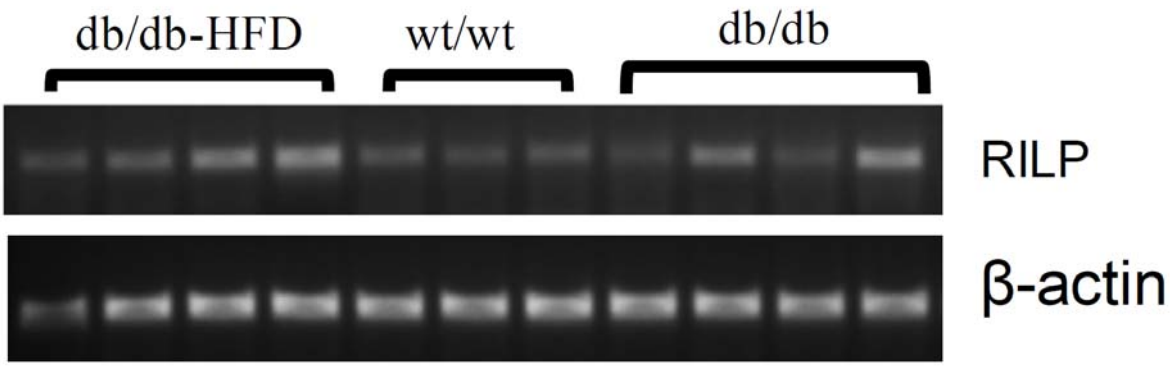

SUPPLEMENTARY DATA

Supplementary Figure 3. (A), INS-1 cells were transfected with mCherry-vector and immunostained with insulin/proinsulin antibody, demonstrating vector did not induce insulin granules clustering. (B), INS-1 cells were transfected with EGFP-RILP, and immunostained with insulin/proinsulin antibody, demonstrating RILP induces insulin granules clustering, and the arrow indicated insulin granules secreted to surface under GSIS condition. (C), INS-1 cells were transfected with GFP-RILP, and immunostained with Chromogranin A (CGA) antibody. (D), INS-1 cells were transfected with mCherry-vector and immunostained with proinsulin antibody, demonstrating vector did not influence proinsulin staining signals.

SUPPLEMENTARY DATA

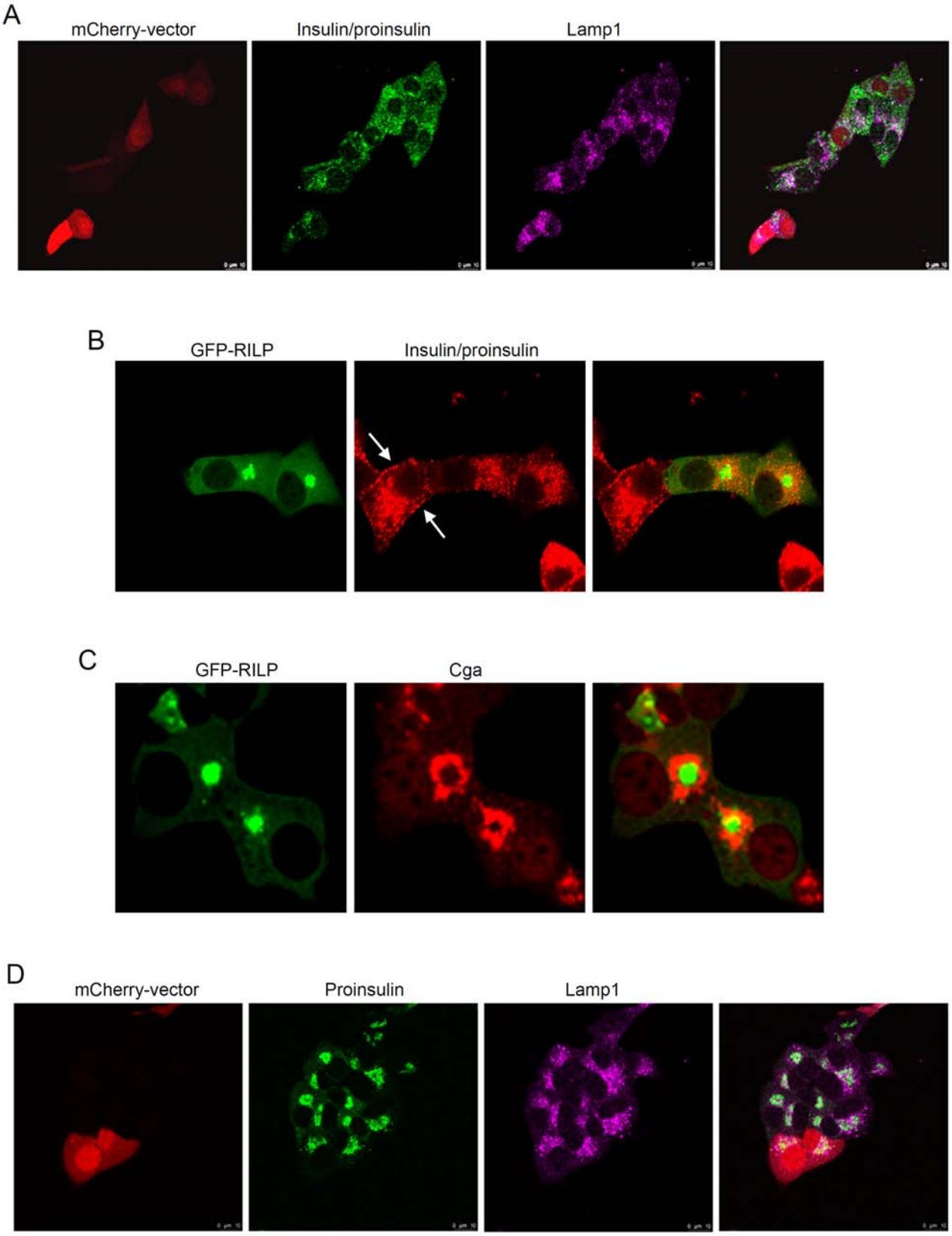

SUPPLEMENTARY DATA

Supplementary Figure 4. (A) and (B), mRNA levels of *Ins1* and *Ins2* retrieved by qPCR from the Min6 cells expressing RILP, indicated over-expression of RILP did not affect the transcription of insulin genes. (C) Min6 cells were infected with Ad-shRNA-RILP, cell lysates were subjected for Western-blot with RILP antibody, indicating both shRNA-RILPs sufficiently deplete the endogenous RILP protein. (D), Min6 cells were infected with Ad-shRNA-Rab7, cell lysates were subjected for Western-blot with Rab7 antibody, indicating shRNA-Rab7-2 sufficiently deplete the endogenous Rab7 protein.

SUPPLEMENTARY DATA

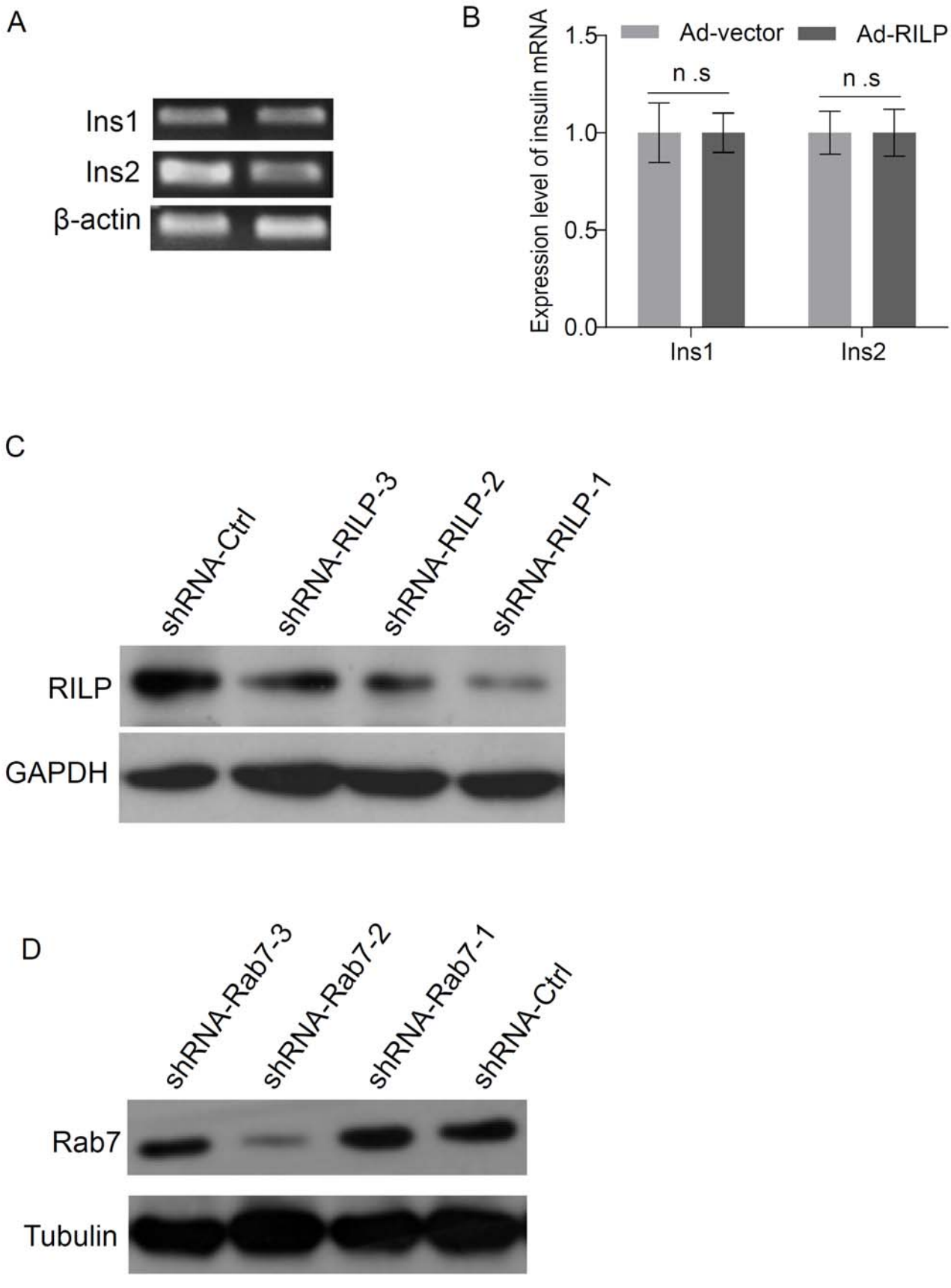

SUPPLEMENTARY DATA

Supplementary Figure 5. (A), INS-1 cells were transfected with mCherry-vector and immunostained with insulin/proinsulin and Lamp1 antibodies, demonstrating a small pool of insulin granules associates with the lysosomes. (B), mCherry-vector transfected INS-1 cells were treated with 20mM NH4Cl, then immunostained with insulin/proinsulin and Lamp1antibodies, demonstrating NH4Cl treatment increases the co-localization of insulin/Lamp1. (C), INS-1 cells were transfected with GFP-RILP(199-401aa), and immunostained with insulin/proinsulin antibody. Demonstrating insulin granules associate with RILP-containing compartments. Colocalization of insulin with Lamp1 in images was analyzed by ImageJ software and expressed as Pearson's correlation coefficient (R).

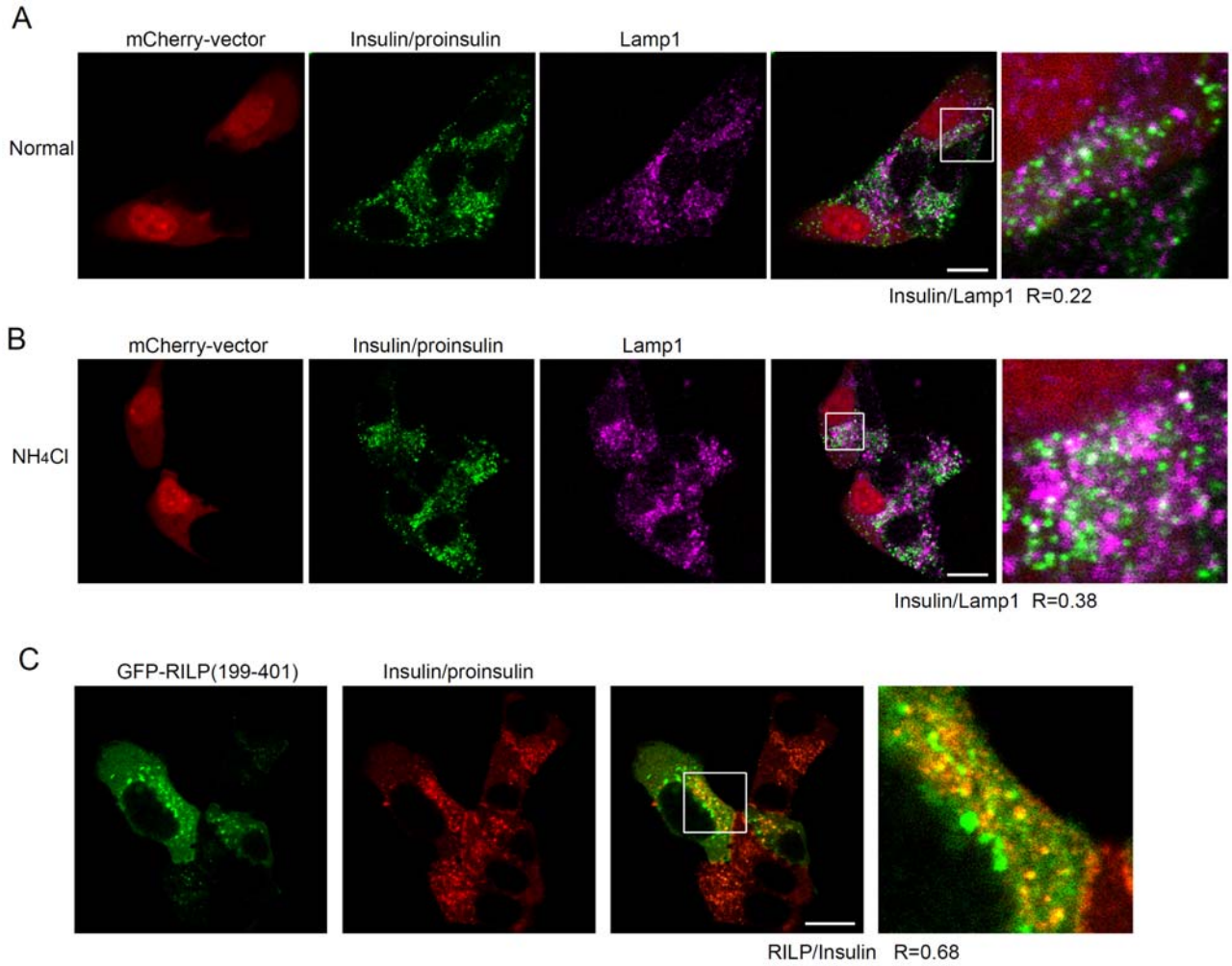

SUPPLEMENTARY DATA

Supplementary Figure 6. (A), ATG7 was knocked down by si4 and si5 siRNA targeting ATG7. (B), ATG7 knockdown has no major effects on proinsulin degradation mediated by Ad-RILP. (C) and (D), cell lysates of INS-1 cells expressing Ad-RILP were processed for Western-blot to detect LC3II/LC3I using LC3 antibody, showing over-expression of RILP has no effects on the ratio of LC3II/LC3I under different conditions. (E) and (F), cell lysates of INS-1 cells expressing Ad-RILP were processed for Western-blot to detect LC3II/LC3I using LC3 antibody, showing over-expression of RILP has no effects on the ratio of LC3II/LC3I upon chloroquine treatment. (G), INS-1 cells were co-transfected with GFP-RILP and mCherry-LC3, then immuno-stained with insulin/proinsulin antibody, showing RILP did not induce co-localization of insulin granules with autophagosomes marked by LC3.

SUPPLEMENTARY DATA

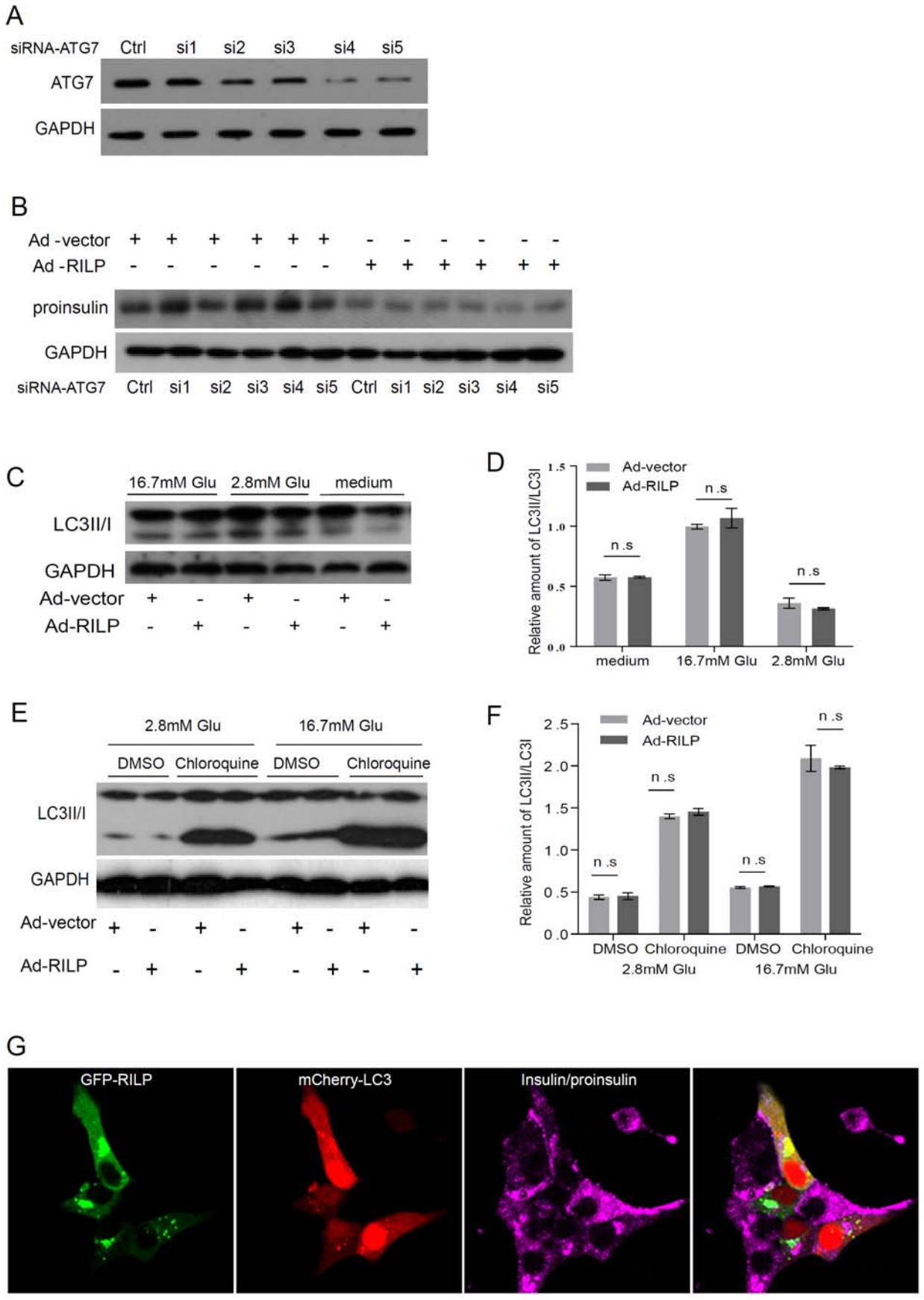

SUPPLEMENTARY DATA

Supplementary Figure 7. (A) 293t cells were transfected with flag-tagged Rab proteins, respectively. The resulted cell lysates were subjected for GST-pulldown assay with GST-RILP, and Rab proteins interacting with RILP were detected by Western-blot and the arrow indicated Rab26 interacts with RILP. (B) Min6 cells were infected with Ad-shRNA-Rab26, the knockdown efficiency was examined by RT-PCR, shRNA-Rab26-4 was used for the further experiments indicated in the text.

SUPPLEMENTARY DATA